Supplementary Materials for

KDM6B cooperates with Tau and regulates synaptic plasticity and cognition via inducing VGLUT1/2

Yanan Wang[1], Nitin Khandelwal[2], Shuiqiao Liu[1], Mi Zhou[1], Lei Bao[1], Jennifer E Wang[1], Ashwani Kumar[3], Chao Xing [3,4,5], Jay Gibson[2] and Yingfei Wang[1,6,7]*

**Corresponding author.*
Email: Yingfei.Wang@UTSouthwestern.edu

This PDF file includes:

Methods
Figs. S1 to S9
Tables S1 to S3
References

Other Supplementary Materials for this manuscript include the following:

Data S1 to S2

METHODS

Reagents, antibodies, and plasmids

Chemicals were purchased from Sigma-Aldrich unless otherwise indicated. TTX and picrotoxin were purchased from Tocris Bioscience. Information of primary antibodies has been summarized in Supplemental Table 1. C-terminal human *KDM6B* cDNA with 3x Flag tag and SV40 nuclear localization signal (NLS) at its N-terminus was generated by PCR using MSCV JMJD3 (Addgene, #21212) or MSCV JMJD3 mutant (Addgene, #21214) as a template and cloned into pLL-Ubc vector, which was modified from pLL3.7 (Addgene, #11795) by replacing the CMV promotor with human Ubc promoter and removing the LoxP site. C-terminal human *KDM6A* cDNA with 3x Flag tag and SV40 NLS at its N-terminus was generated by PCR and cloned into pLL-Ubc vector. Mouse Tau cDNA was generated by PCR and cloned into PRK5 vector. The cDNAs of *Slc17a7* and *Slc17a6* were generated by PCR and cloned into pLL-Ubc vector, respectively. The oligonucleotide sequences of mouse KDM6A shRNAs are: KDM6A-sh1, 5'-AGTTAGCAGTGGAACGTTATG-3'; KDM6A-sh2, 5'-GCTACGAATCTCTAATCTTAA-3'. The oligonucleotide sequences of mouse Tau shRNAs are: Tau-sh1, 5'-GCTAGATAGATAGGGCATACA-3'; Tau-sh2, 5'-TGGAGCAGAAATTGTGTATAA-3'. The oligonucleotide sequence of scrambled control shRNA is 5'-TTCTCCGAACGTGTCACGT-3'. All constructs were verified by DNA sequencing.

Animals

Mice were housed in a room at 24 °C in a 12 h light/dark cycle with access to food and water ad libitum. *LoxP*-flanked *Kdm6b* (*Kdm6b*$^{fl/fl}$) mice were kindly provided by Dr. Stuart H. Orkin (Harvard Medical School). PCR-based genotyping of *Kdm6b*$^{fl/fl}$ mice was performed using

genomic DNA isolated from the tail or cortex with a forward primer (5'-CCTGTCTGTGATTTTTGCCCC-3') and a reverse primer (5'-CACAGGAATGCCGACGAAAT-3'). Two PCR products with 180 bp and 250 bp were amplified from the wild-type and floxed *Kdm6b* alleles, respectively. *Kdm6b*$^{fl/fl}$ (C57BL/6) mice were crossed with CamKIIα-iCre transgenic mice (EMMA, EM 01153) [1, 2] to produce *Kdm6b*$^{fl/fl}$;CamKIIα-*iCre*+ mice. CamKIIα-*iCre* mice were genotyped with primer1 (5'-TCGTCAGTCAAGCCGGTTC-3'), primer2 (5'-AATCATGCTGCACACCTCCC-3'), and primer3 (5'-CAGGTTTTGGTGCACAGTCA-3'). A 320-bp PCR product is expected to be amplified from the wild-type allele using primers 1 and 2 and a 191-bp PCR product is expected from the CamKIIα-iCre allele using primers 1 and 3. *Kdm6b*$^{fl/fl}$ mice were crossed with Nestin-Cre mice (JAX 003771) to produce *Kdm6b*$^{fl/fl}$;Nestin-Cre+ mice. Nestin-Cre mice were genotyped with primer1 (5'-TTGCTAAAGCGCTACATAGGA-3'), primer 2 (5'-GCCTTATTGTGGAAGGACTG-3'), and primer 3 (5'-CCTTCCTGAAGCAGTAGAGCA-3'). A 246-bp PCR product is expected to be amplified from the wild-type allele using primers 1 and 2 and another 150-bp fragment is expected to be amplified from the Nestin-Cre allele using primers 2 and 3. Thy1-eGFP mice were from The Jackson Laboratory (JAX# 007788). Male mice were used for all biochemical experiments, electrophysiology recordings, and behavioral tests. Experimental procedures were performed with the approval of the Institutional Animal Care and Use Committee at University of Texas Southwestern Medical Center.

Mouse neuronal cultures

Primary cortical neurons were cultured as described previously with modifications [3]. Briefly, mouse cortexes were isolated from embryos at embryonic day 18 (E18), kept separately in cold

HBSS (Gibco, 14175) and incubated for 15 min with 20 units/mL of papain (Worthington, LK003178) at 37 °C. Dissociated cells were suspended in plating media (DMEM supplemented with 20% horse serum) and plated at a density of 6×10^4 per well onto poly-L-lysine–coated 18-mm coverslips (Fisherbrand, 12-545-100) in a 12-well plate (Thermo Scientific, 150628) or 6×10^5 per well on a 6-well plate (Thermo Scientific, 140675). Neurons were incubated for 4 h before replacing with maintaining media containing Neurobasal A medium (ThermoFisher Scientific, 10888022) supplemented with 2% N21-MAX supplement (R&D Systems, AR008), 1% GlutaMax (ThermoFisher Scientific, 35050061), and 1% penicillin/streptomycin (ThermoFisher Scientific, 15140122), and cultured at 37 °C in a 5% CO_2/95% air incubator, by changing half of media every 2–3 days with fresh maintaining media. Neurons were infected with lentiviruses encoding KDM6A shRNAs or at DIV 5 to 7 and used for experiments at DIV14 to 18. Primary astrocytes and microglial cells were also cultured separately from P0-P2 pups as described previously [4-6].

Neuron transfection

To conduct the spine number counting and dendritic morphology assay, neurons were transfected using Lipofectamine 2000 (ThermoFisher, 11668019) according to the manufacture's protocol. Briefly, at DIV 6, neurons were transfected with 1 μg of pLL-Ubc-eGFP plasmid using 1.5 μl of Lipofectamine reagent. DNA-lipofectamine complexes were added to the neurons and incubated for 2 h, after which the transfection media was replaced with conditioned neuronal media. Neurons at DIV 18 were used for spine number counting and dendritic morphology analysis.

Lentivirus production

Lentivirus production was performed as described previously with modifications [3]. In brief, HEK293T cells were cultured in Dulbecco's modified Eagle's medium (DMEM) (Sigma, D6429) supplemented with 10% fetal bovine serum (FBS) (Sigma, 12306C), and transiently transfected with 5.4 μg transducing vector, 6 μg psPAX2, and 1.8 μg pMD2.G using 13.2 μL of polyethyleneimine (Fisher, NC1038561, 5 mg/ml). Lentivirus was harvested 48 h and 72 h after transfection and concentrated by ultracentrifugation (100, 000 g) for 1 h to a final concentration of 10^8 infection units/ml in phosphate buffered saline (PBS).

Immunoblotting

Immunoblotting was performed as described previously [3]. Brain tissues or cultured cells were homogenized in RIPA buffer (50 mM Tris-HCl, pH 7.4, 150 mM NaCl, 2 mM EDTA) containing 0.5 % sodium deoxycholate, 0.1% SDS, 1 mM PMSF, 1 mM Na_3VO_4, 1 mM NaF, 1 mM DTT and protease inhibitor cocktail. Samples were centrifuged at 12,000 x g for 20 min at 4 °C to remove debris. Lysates (50 μg of protein from tissue, 10 μg of protein from cell cultures) were separately by SDS-PAGE and transferred to nitrocellulose membrane (Bio-Rad, 1620115). The membrane was immunoblotted with antibodies and immunoreactive bands were visualized by enhanced chemiluminescence (Pierce, 37069). Data were quantitated by using NIH ImageJ.

Co-immunoprecipitation (Co-IP)

HEK293T cells were cultured in DMEM supplemented with 10% FBS, and transiently transfected with 1 μg of plasmid DNA using 1 μL of polyethyleneimine (5 mg/ml). After 36 hours, cells were lysed in the lysis buffer (50 mM Tris-HCl, pH7.5, 150 mM NaCl, 1% Triton X-100) plus protease inhibitor cocktail and centrifuged at 16,000 g for 10 min at 4 °C. The supernatant of cell lysates

was precleared by incubating at 4 °C for 1 h with protein A/G PLUS-Agarose beads (Santa Cruz, sc-2003). Precleared samples were incubated with respective antibodies overnight at 4 °C. Normal mouse IgG (Santa Cruz, sc-2025) was used as a negative control. The immune complexes were incubated with protein A/G PLUS-Agarose beads for 4 h at 4 °C. After washing four times with lysis buffer, the bound proteins were fractionated by SDS-PAGE, followed by immunoblotting, or eluted with 0.5 mg/ml 3×Flag peptide, followed by mass spectrometry analysis.

5-Bromo-2'-deoxyuridine (BrdU) injection

2-month-old mice were injected twice with BrdU (Sigma, B5002; i.p., 100 mg/kg body weight, 1 time/6 h) before perfusion. Mouse brain was collected and sectioned for BrdU immunostaining to analyze cell proliferation.

Immunohistochemistry and immunocytochemistry

Immunostaining was performed as described previously with modifications [7]. Briefly, mice were deeply anesthetized with 5% isoflurane and perfused with PBS followed by ~30 ml 4% paraformaldehyde (PFA). Brains were post-fixed overnight in 4% PFA at 4 °C and dehydrated using 30% sucrose at 4 °C for two days. Brain tissues were embedded in optimal cutting temperature compound, rapidly frozen, and cut into 30 or 100 μm (for Thy-1 GFP mice)-sections. Sections were blocked, permeabilized in PBS containing 0.3% Triton X-100, 10% donkey serum and 1% BSA for 1 h at room temperature and incubated at 4 °C overnight with primary antibodies in PBS containing 1% donkey serum and 1% BSA. After washing with PBS, sections were incubated at room temperature for 1 h with secondary antibodies. Cultured cells were fixed with 4% PFA for 15 min at room temperature, washed with PBS, permeabilized with 0.2% Triton X-

100 for 10 min, blocked with 10% BSA for 1 h, and labeled with primary antibodies overnight at 4°C. After washing with PBS, cells were incubated with secondary antibodies for 1 h at room temperature. Nissl staining was performed as described previously [7].

Neuron morphometric analysis

The axon length was measured using ImageJ loaded with a plugin of Simple Neurite Tracer in Tau staining images of neurons (DIV 3) acquired by Zeiss microscope. The images of dendritic tree and spines were taken from DIV 18 neurons. The images of dendritic tree were obtained using Zeiss LSM 880 confocal microscope at 20x magnification, under a Z-stack program. To measure the complexity of dendritic arbor, the EGFP fluorescence signals of the dendritic tree were thresholded and binarized. Sholl analysis was performed with 20 mm intervals and a total number of crossings with circles was quantified. The spines were imaged with Zeiss LSM 800 confocal microscope at 60x magnification with 3x zoom in, under a Z-stack program. Spines on the secondary/tertiary branches were quantified with ImageJ software.

Subcellular fractionation of mouse brain

Mouse brain subcellular fractions were prepared as described previously with modifications [8]. All procedures were performed at 4 °C and buffers or solutions contained protease inhibitor cocktail and phosphatase inhibitors (50 mM NaF, 1 mM sodium orthovanadate, 20 mM β-glycerophosphate). Briefly, brain tissues were homogenized in 10 volumes of HEPES-buffered sucrose (0.32 M sucrose, 4 mM HEPES/NaOH, pH 7.4) with a glass-Teflon homogenizer. Homogenates were centrifuged at 1,000 × g for 10 min to remove nuclear and other cell debris and collect the supernatant (Sn1). Sn1 fraction was then centrifuged at 10,000 × g for 15 min to obtain

the crude synaptosomal fraction (P2) and supernatant (Sn2). The P2 pellet was resuspended in HEPES-buffered sucrose, carefully layered on top of a discontinuous gradient containing 0.8 –1.0 –1.25 M sucrose (top to bottom), and centrifuged at 100,000× g for 30 min. The gradient centrifugation yielded a synaptosome fraction at the 1.0/1.25 sucrose interface. Synaptosome fraction was collected and added the equal volume of HEPES-buffered sucrose, followed by centrifugation at 20,000 g for 15 min to collect the synaptosome pellet. The synaptosome pellet was incubated with 1% Triton X-100 in 50 mM HEPES/NaOH (pH 8.0) at 4 °C for 30 min and subjected to centrifugation at 25,000× g for 1 h to collect the pellet (postsynaptic membrane fraction). 12 μg of total protein, 4 mg of synaptosome and 4 mg postsynaptic membrane fraction proteins were used for immunoblotting.

Quantitative reverse transcription-polymerase chain reaction (qRT-PCR) assay

Total RNA was isolated from indicated tissues or cultured cells using TRIzol reagent (Invitrogen, 15596018), treated with DNase I (Invitrogen, AM1906), and reverse-transcribed using the iScript cDNA Synthesis Kit (Bio-Rad). Real-time PCR was performed by a CFX-96 Real time System (Bio-Rad) using iTaq Universal SYBR Green Supermix (Bio-Rad) with primers listed in Supplemental Table 2. The fold change in target mRNA expression was calculated based on the threshold cycle (Ct) as $2^{-\Delta(\Delta Ct)}$, where $\Delta Ct = Ct_{target} - Ct_{b\text{-}actin}$.

RNA-seq

KDM6B KO and WT neurons were collected at DIV 14. Total RNA was isolated using TRIzol reagent according to the manufacture's protocol and treated with DNase I. The quality of total RNA was confirmed with a RNA integrity number score 8.5 or higher by the Agilent TapeStation

4200. 0.2 μg of DNA-free total RNA was used for library preparation with KAPA mRNA HyperPrep Kit (Kapa Biosystems, KK8580). Briefly, mRNA with polyA was purified and fragmented before strand-specific cDNA synthesis. cDNAs were end repaired and A-tailed, and the indexed sequencing adapters were ligated. After the cDNAs were amplified by PCR and purified with AmpureXP beads, the samples were sequenced on the Illumina NextSeq 500 with the read configuration as 76 bp, single end. Each sample had approximately 25 million to 35 million reads. Bioinformatics were performed as described previously [9].

Chromatin immunoprecipitation (ChIP)-qPCR assay

ChIP-qPCR was performed as previously described [3, 9]. Primary neurons (DIV 14) were cross-linked with 1% formaldehyde for 10 minutes at room temperature and quenched in 0.125 M glycine for 5 min at room temperature. Chromatin was then isolated using SimpleChIP Enzymatic Chromatin IP Kit (Cell Signaling Technology, 9003), digested to 150-300 bp in length, and subjected to immunoprecipitation with indicated antibodies in the presence of ChIP grade protein G magnetic beads. After protein-DNA cross-link reversal, DNA was purified using DNA purification spin columns and subjected to qPCR. The primers used for ChIP-qPCR are listed in Supplemental Table 3.

Electron microscopy analysis

Electron microscopy studies were carried as described previously [7]. Briefly, anesthetized mice were perfused transcardially with 0.1 M phosphate buffer containing 2% glutaraldehyde and 2% PFA. Brains were post-fixed for 1 h at 25 °C and then overnight at 4 °C. Ultrathin sections of the cortex were examined with a JEM 1400 Plus transmission electron microscope (JEOL USA)

equipped with a LaB6 source operated at 120 kV. Images were collected with an AMT camera system (AMT Imaging). Synapses were identified by ultrastructural specializations, including alignment of presynaptic and postsynaptic membranes, presynaptic and postsynaptic thickenings, and clusters of synaptic vesicles. The length of PSD, density of synaptic vesicles within 0.04 mm^2 areas surrounding active zones or adjacent to terminals were quantified by investigators who were unaware of mouse genotypes using Image J.

Electrophysiological recording in brain slices

Cortical slices were prepared as described previously [10]. Brains were isolated from anesthetized male mice (3 weeks old) and chilled in ice-cold dissection buffer containing: 110 mM Choline-Cl, 2.5 mM KCl, 1.25 mM NaH_2PO_4, 25 mM $NaHCO_3$, 25 mM Dextrose, 3 mM Ascorbic Acid, 3 mM Sodium Pyruvate, 7 mM $MgCl_2$, 0.5 mM $CaCl_2$, and 0.2 mM Kyneuric Acid, with 7.3-7.4 pH and 280-285 mOsm osmolality. Coronal brain slices containing cortex (300 μm thickness) were cut in a semi-frozen dissection buffer using a VTS 1200S vibratome (Leica) and incubated in a regular ACSF (bubbled with 5% CO_2 and 95% O_2) containing 125 mM NaCl, 3 mM KCl, 2 mM $MgCl_2$, 2 mM $CaCl_2$, 1.25 mM NaH_2PO_4, 25 mM $NaHCO_3$, and 10 mM dextrose with 7.3-7.4 pH and 295-300 mOsm osmolality, at 35 °C for 30 min and then at room temperature (25 ± 1°C) for additional 30 min before recordings. Slices were placed in the recording chamber which was superfused (2 mL/min) with regular ACSF (saturated with 95% O_2/5% CO_2) at 30 °C. Layer 5 pyramidal neurons were visualized with infrared optics using an upright microscope with a 40x water-immersion lens (Axioskop 2 Plus, Zeiss) and infrared-sensitive CCD camera (Hamamatsu, C2400-75) for whole-cell recording with glass pipettes (resistance of 5-6 MΩ). Data were acquired by a MultiClamp 700B amplifier and a 1440A digitizer (Molecular Device). For recordings of

sEPSCs (spontaneous excitatory post-synaptic currents), layer V neurons were clamped at -70 mV with the pipette solution containing 130 mM K-Gluconate, 6 mM KCl, 3 mM NaCl, 10 mM HEPES, 0.2 mM EGTA, 4 mM ATP-Mg, 0.4 mM GTP-Tris, and 14 mM phosphocreatine-Tris (pH 7.40, 285-290 mOsm). Cells were excluded if resting membrane potential was more positive than -60 mV or if series resistance was more than 20 MΩ and/or fluctuated more than 20% of initial values. All recordings were done at 30 °C. In voltage clamp, a single -10 mV voltage step (500 ms duration) was applied to measure input resistance. In current clamp, incremental current steps of 50 mA (500 ms duration, up to 350 mA) were applied and number of action potentials were plotted for a "firing versus current injection" curve. sEPSCs were collected at -70 mV holding potential and then analyzed using Mini Analysis Program (Synaptosoft) after low-pass filtering (1 kHz frequency cut-off).

Electrophysiological recording in neuron cultures

Whole-cell voltage clamp was used to record miniature excitatory post-synaptic currents (mEPSCs) in neurons at 13-15 DIV. Cells were continuously perfused with external recording solution containing: 145 mM NaCl, 3 mM KCl, 3 mM $CaCl_2$, 2 mM $MgCl_2$, 8 mM dextrose, and 10 mM HEPES (pH 7.3, 295-300 mOsm). The neurons were clamped at -70 mV with the patch electrodes (3-5 MΩ) filled with an internal solution containing: 125 mM K-gluconate, 15 mM KCl, 10 mM HEPES, 0.2 mM EGTA, 4 mM Mg-ATP, 0.3 mM Na-GTP, and 10 mM Na-phosphocreatine (pH 7.30, 290-300 mOsm). To measure mEPSCs, 1 μM TTX (Tocris, 1069) and 100 μM picrotoxin (Tocris, 1128) were added to the external recording solution. Cells were excluded if resting membrane potential was more positive than -60 mV or if series resistance was more than 20 MΩ and/or fluctuated more than 20% of initial values. mEPSCs were analyzed using

the Template Search tool of the Clampfit 10.2 software (Molecular Devices). To create the template, several well-shaped mEPSCs traces were picked from recording in WT neurons and averaged to the template window.

Animal behavioral tests

Animal behavioral tests were performed as previously [11]. For locomotor activity test, mice were placed in a chamber (45 x 45 x 15 cm) and their movement in the central (15 x 15 cm) and peripheral zones of chamber was monitored for 5 min using an overhead camera and tracking software (EthoVision, Noldus). For the elevated plus maze test, mice were first placed in the central zone of the plus maze that has two opposing wall-closed arms and two open arms (5 cm width x 66 cm length each). Mouse movement was recorded for 15 min using an overhead camera and tracking software (EthoVision, Noldus). The time mice spent in the open arms, the immobility times and movement distance within 5 minutes time window was quantified automatically.

For working memory test, mice were placed at the center of a Y-shaped maze with three arms (35 cm length) defined as A, B and C respectively. Mice were allowed to move freely through the maze for 8 min. The total arm entry number and series of arm entries were recorded. Nonoverlapping entrance sequences (e.g., A-B-C, B-C-A) were defined as spontaneous alternations.

For rotarod test, mice were assessed for their ability to maintain balance on a rotating bar with accelerated speeds from 4 to 40 rpm over a period of 4-min. Latency to fall from the rod was recorded. Each mouse was given 3 trials per day for 2 days with an interval of 60 min. Tail suspension test (TST) was performed as described previously [12]. Immobility time within a 6-minute time window was measured directly.

Social interaction was measured in a black plexiglass rectangular box that consists of 3 interconnected chambers as described previously [13]. In habituation, mouse was allowed to explore 3 chambers for 10 min. If it showed a preference to one side of the chamber, the mouse was excluded from the test. In the first phase, mouse was placed in the center chamber with both gates to the side chambers closed. A stranger wild-type mouse (S1) was then introduced into the cage of one chamber while the other chamber had an empty cage (E). After opening both gates, the test mouse was monitored for the distance to the S1 and E cages for 10 min. In the second phase, the test mouse was placed in the center chamber with both gates closed; the S1 mouse was placed in the E cage and a second stranger wild-type mouse (S2) was placed in the previous S1 cage. The test mouse was allowed for free exploration and monitored for the distance to either cage for 10 min. The time mice spent on each cage within 2 cm was quantified as social interaction time.

Novel object recognition test was measured as described previously [14]. Briefly, in the familiarization stage, mouse was put into a box (45 x 45 x 15 cm) with two identical tower of Lego bricks. Mouse exploring time on both objects was recorded by stopwatches until reaching either 20 s of total exploration time on objects or 10 min of total time in the box. After 4 hours, one of Lego bricks was replaced by a falcon tissue culture flask filled with sand. Mouse exploring time on both objects was again recorded until reaching either 20 s of total exploration time on objects or 10 min of total time in the box. The exploring time on the single object during the familiarization or the novel object during the test was calculated and presented as % of total exploring time.

Contextual fear conditioning was measured in the Coulbourn Habitest chambers and analyzed by the FreezeFrame software (Coulbourn Instruments). In training time, mice were placed in the conditioning chamber for 120-s habituation and then subjected to parings of conditioned stimulus (an auditory cue) and an unconditioned stimulus with three sets of electric foot shocks (2 s, 0.5

mA, inter-trial interval of 60-90 s). Freezing time after each shock was recorded to determine the capability of animals to sense and escape from foot shock. Animals were removed from the chamber 30 s after the training. 24 hours later, mice were placed back to the same conditioning chamber for 5 minutes but without foot shocks. The freezing time was monitored and quantified.

Statistics and reproducibility

Statistical analysis was performed using GraphPad Prism software. Two-tailed unpaired Student's t-test was used to compare data from two groups. One-way ANOVA with Tukey's or Dunnett's multiple comparisons was used as indicated to compare data from more than two groups. Two-way ANOVA with Tukey's or Sidak's multiple comparisons was used as indicated in behavioral and electrophysiological studies with more than two parameters. "*n*" represents the number of animals or cultures tested. Data were presented as mean ± s.e.m. $P < 0.05$ is considered significant. All experiments were repeated at least three times independently with similar results.

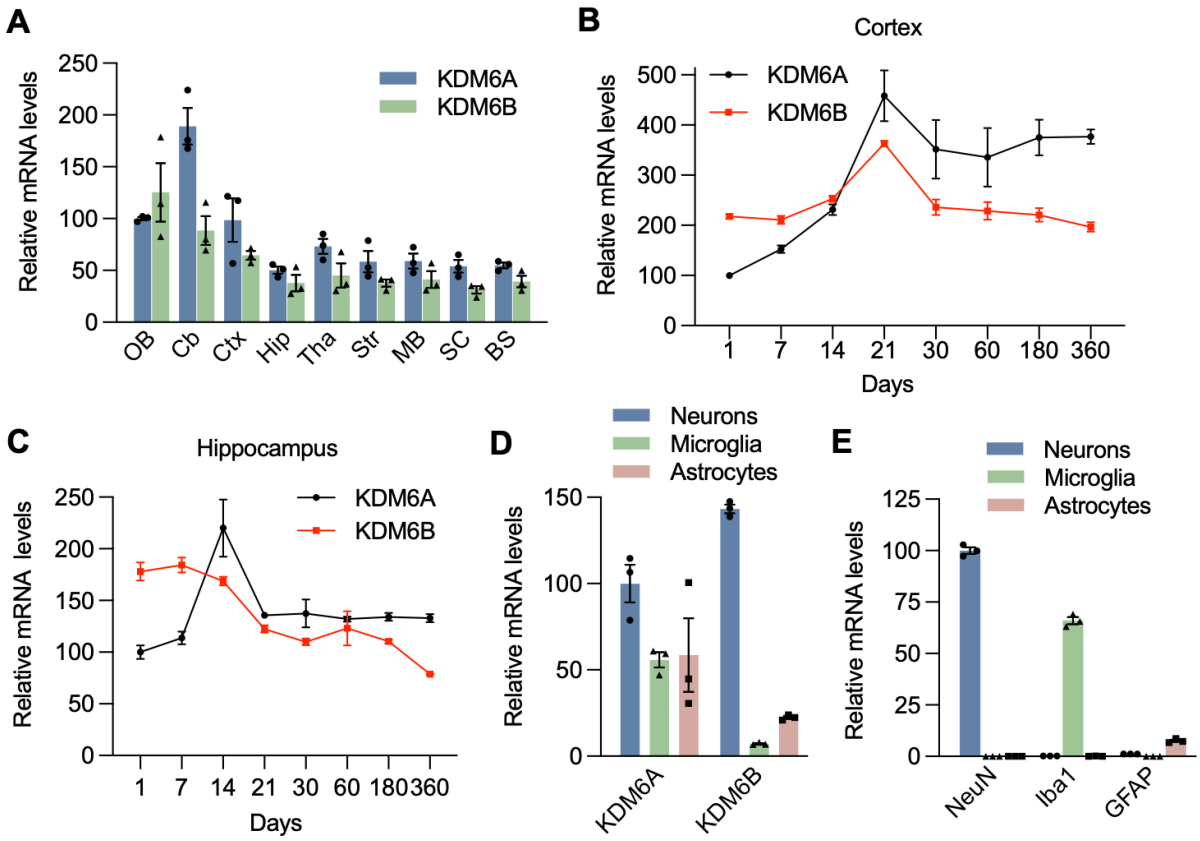

Fig. S1. Spatial and temporal expression of KDM6B in mouse brain.
(**A**) Analysis of KDM6A and KDM6B mRNAs in different brain regions from 2-month-old male mice. OB, olfactory bulb; Cb, cerebellum; Ctx, cortex; Hip, hippocampus; Tha, thalamus; Str, striatum; MB, middle brain; SC, spinal cord; BS, brain stem. n = 3 mice each group. (**B**, **C**) Analysis of KDM6A and KDM6B mRNAs in the cortex (**B**) and hippocampus (**C**) regions of mice with different ages. n = 3 mice each group. (**D**) Analysis of KDM6A and KDM6B mRNAs in primary cultured mouse neurons, astrocytes, and microglia. n = 3 biological replicates in each group. (**E**) Analysis of NeuN, Iba1 and GFAP mRNAs in primary mouse neurons, astrocytes, and microglia. n = 3 biological replicates in each group. Relative mRNA levels were normalized by β-actin. Data were presented as mean ± s.e.m.

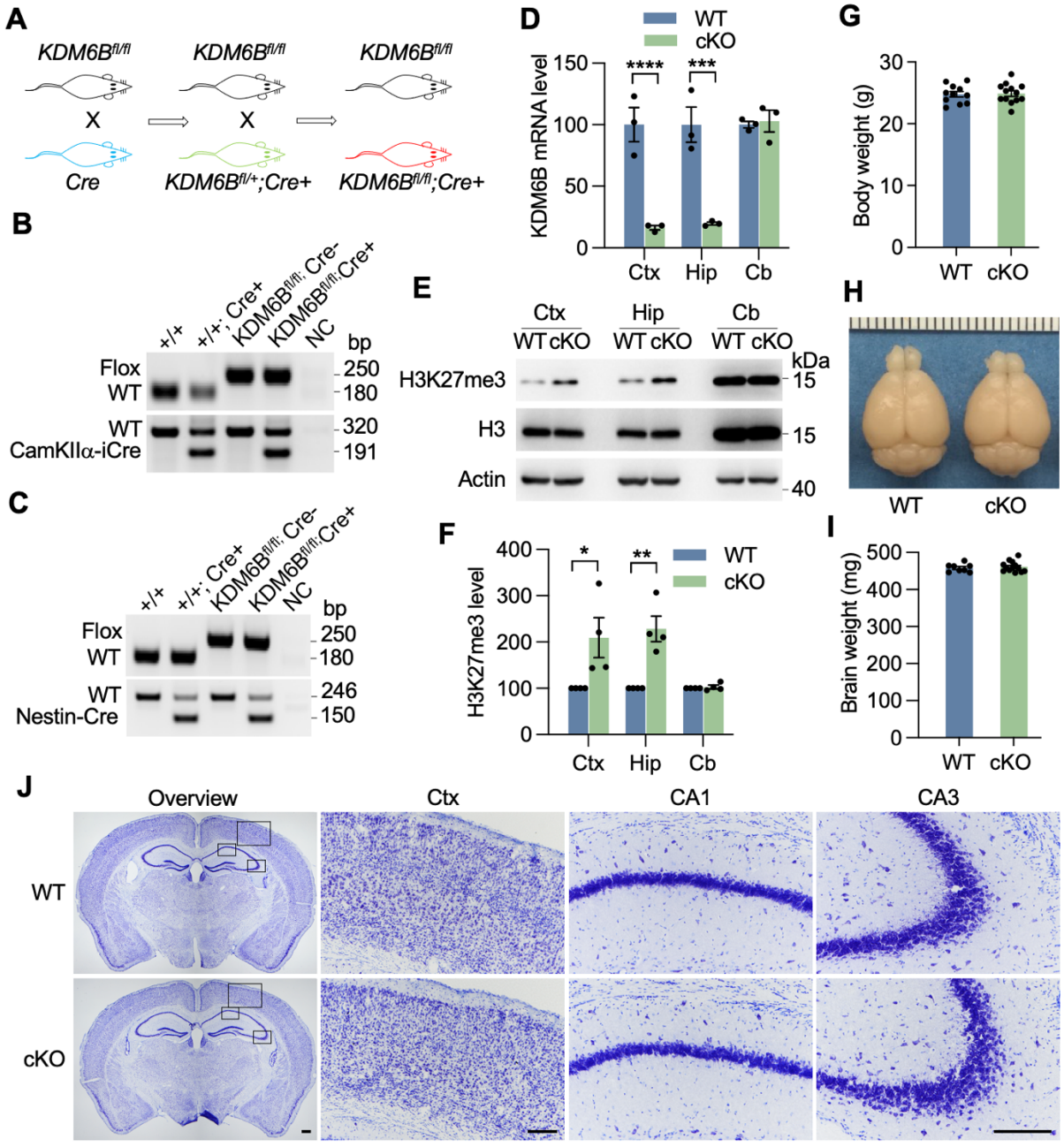

Fig. S2. Effect of KDM6B cKO on mouse brain morphology.
(**A**) The breeding strategy of KDM6B conditional knockout mice. KDM6B$^{fl/fl}$ mice were crossed with CamKIIα-iCre or Nestin-Cre mice. The resulting KDM6B$^{fl/+}$;CamKIIα-iCre+ or KDM6B$^{fl/+}$;Nestin-Cre+ (Cre; KDM6B$^{fl/+}$) mice were crossed with KDM6B$^{fl/fl}$ mice to generate KDM6B$^{fl/fl}$;Cre+ (KDM6B cKO) and KDM6B$^{fl/fl}$ mice. (**B**) PCR genotyping for KDM6B floxed mice with or without CamKIIα-iCre. NC, negative control. (**C**) PCR genotyping for KDM6B floxed mice with or without Nestin-Cre. NC, negative control. (**D**) qRT-PCR analysis of KDM6B mRNA expression in different brain subregions from KDM6B cKO and WT mice. Values of WT mice were taken as 100%. n = 3 biological replicates in each group. Two-tailed Student's t test. (**E**, **F**) Immunoblot analysis of H3K27me3 levels in the cortex (Ctx), hippocampus (Hip), and

cerebellum (Cb) of WT and KDM6B cKO mice. Representative immunoblot images (**E**) and quantification of H3K27me3 intensity normalized to β-actin (**F**). $n = 4$ mice each group. Values of WT mice were taken as 100%. Two-tailed Student's t test. (**G**) Analysis of body weights of 2-month-old KDM6B cKO and WT male mice. $n = 11$ for WT mice, $n = 13$ for KDM6B cKO mice. Two-tailed Student's *t* test. (**H**, **I**) Analysis of brain weights of 2-month-old KDM6B cKO and WT male mice. $n = 8$ for WT mice, $n = 13$ for KDM6B cKO mice. (**J**) Nissl staining analysis of brain gross morphology of 2-month-old KDM6B cKO and WT male mice. The boxed areas in the cortex and hippocampal CA1 and CA3 regions are shown. Scale bar, 100 mm. Data were presented as mean ± s.e.m. *p < 0.05; **p < 0.01; ***p < 0.001; ****p < 0.0001.

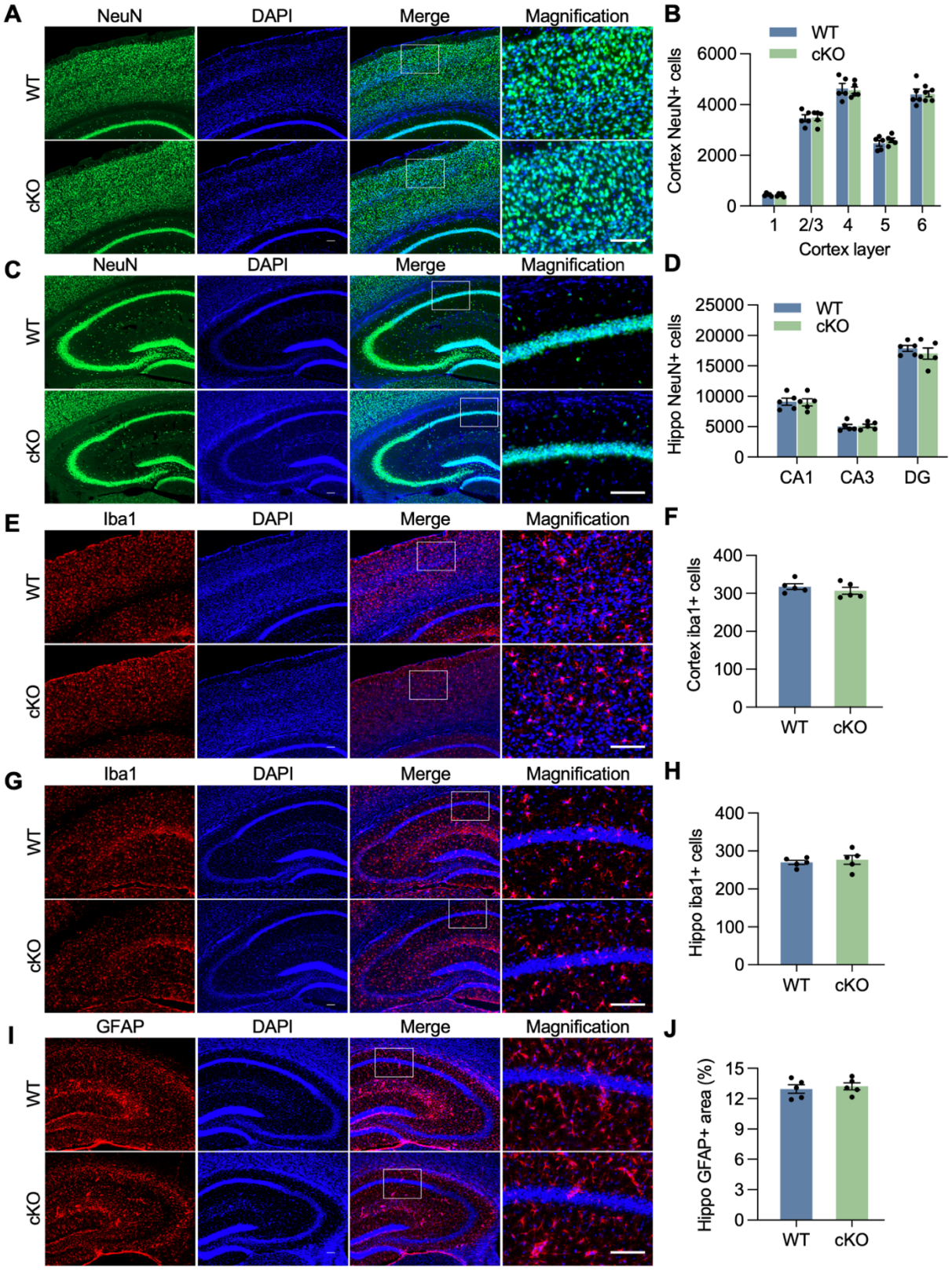

Fig. S3. Effect of KDM6B cKO on mouse brain cells.

(**A-D**) Representative images of NeuN staining in the cortex (**A**) and hippocampus (**C**) of 2-month-old WT and KDM6B cKO mice. NeuN+ cells in the layer I-VI of the cortex (**B**) and hippocampal

CA1, CA3, and DG regions (**D**) were quantified. *n* = 5 mice each group. Scale bar, 100 μm. (**E-H**) Representative images of Iba1 staining in the cortex (**E**) and hippocampus (**G**) of 2-month-old WT and KDM6B cKO mice. Iba1+ cells in the cortex (**F**) and hippocampus (**H**) were quantified. Scale bar, 100 μm. *n* = 5 mice each group. (**I**, **J**) Representative images (**I**) and quantification (**J**) of GFAP staining in the hippocampus of 2-month-old WT and KDM6B cKO mice. Scale bar, 100 μm. *n* = 5 mice each group. Data were presented as mean ± s.e.m.

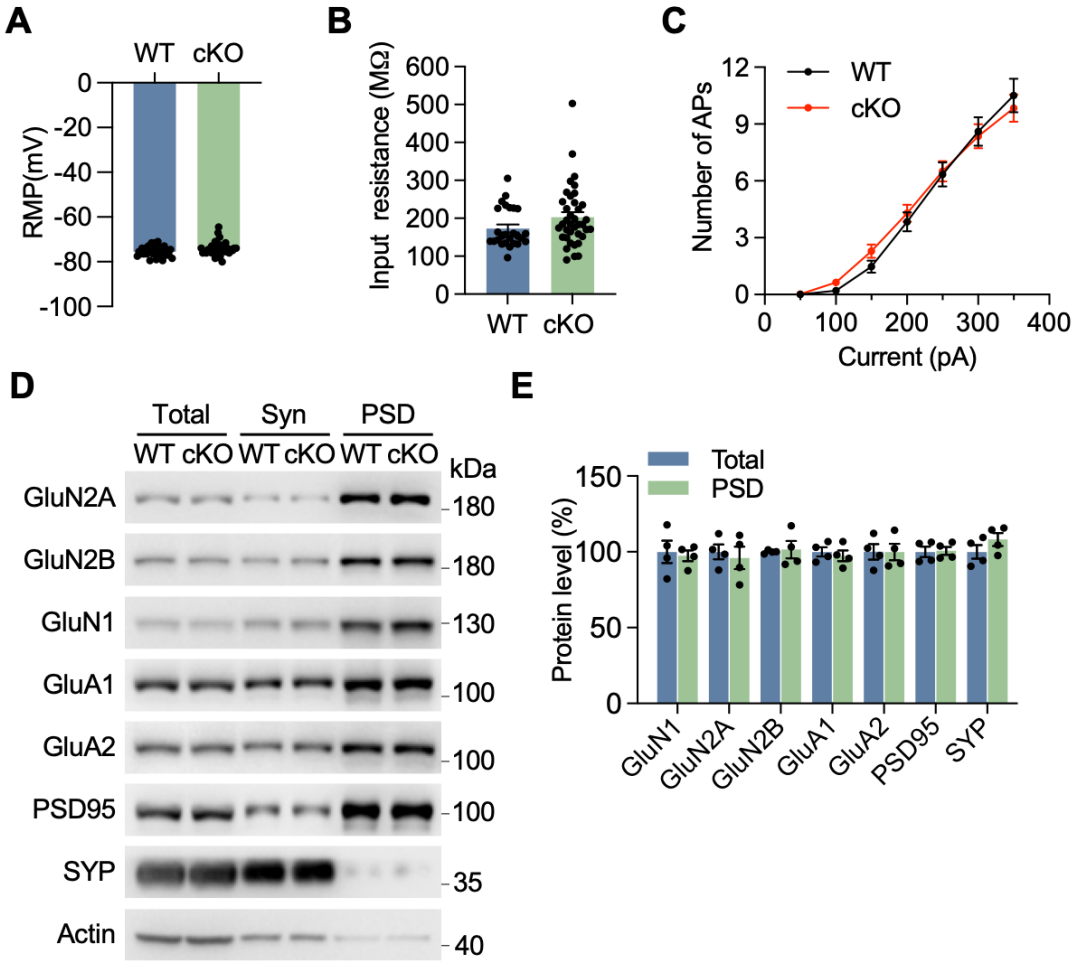

Fig. S4. Effect of KDM6B cKO on neuron activity and postsynaptic protein expression in mouse cortex.

(**A**, **B**) Analysis of resting membrane potential (**A**) and input resistance (**B**) in layer V pyramidal neurons of KDM6B cKO and WT mice. Input resistance was measured at -60 mV. $n = 26$ neurons from 3 WT mice. $n = 38$ neurons from 5 KDM6B cKO mice. (**C**) Analysis of firing rates plotted against increasing injected currents in layer V pyramidal neurons of KDM6B cKO and WT mice. $n = 30$ neurons from 3 WT mice. $n = 48$ neurons from 5 KDM6B cKO mice. Two-way ANOVA with Tukey's multiple comparisons. (**D**, **E**) Immunoblot analysis of postsynaptic proteins in the cortex of KDM6B cKO mice and WT mice. Representative images in homogenates (Total), synaptosomal fraction (Syn), and PSD fraction (**D**). Quantitation of protein intensity (**E**). $n = 4$ mice in each group. Values of WT mice were taken as 100%. Data were presented as mean ± s.e.m.

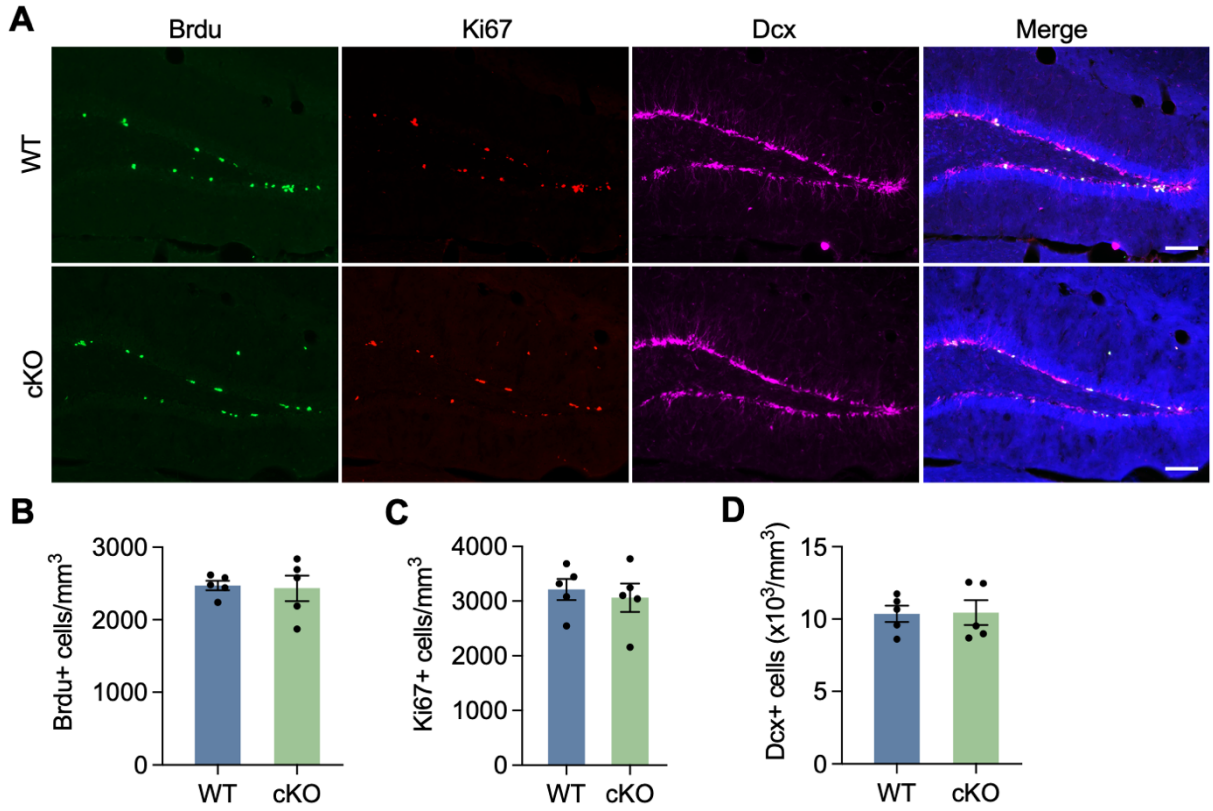

Fig. S5. Effect of KDM6B cKO on adult neurogenesis in mice

(**A-D**) Immunostaining analysis of BrdU-, Ki67-, and Dcx-labeled cells in the subgranular zone (SGZ) region of KDM6B cKO and WT mice. Representative images (**A**). Scale bar, 100 mm. Stereological quantification of SGZ $BrdU^+$ (**B**), $Ki67^+$(**C**) and Dcx^+ (**D**) cells. n = 5 mice each group. Data were presented as mean ± s.e.m.

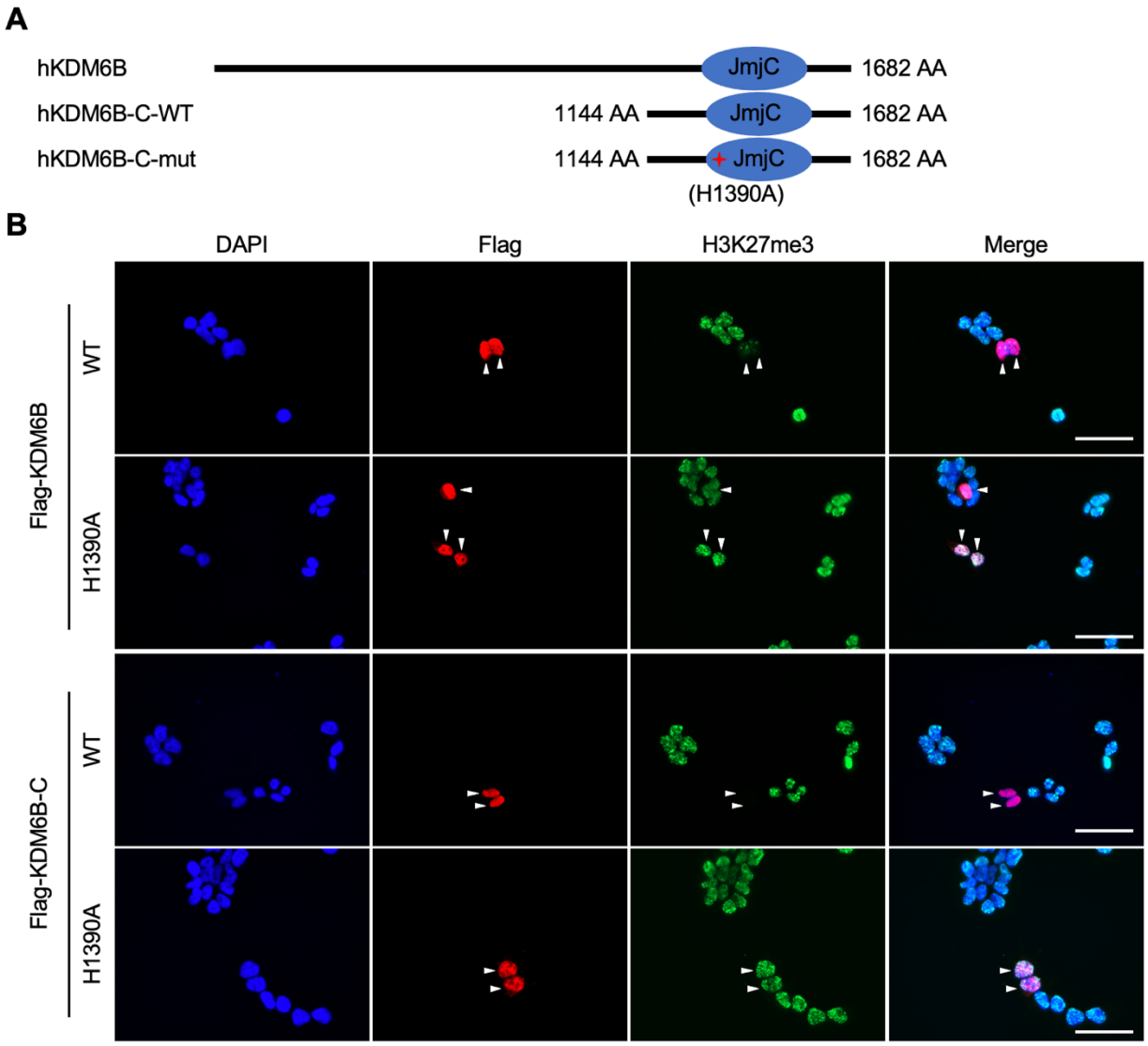

Fig. S6. C-terminal KDM6B is sufficient to reduce H3K27me3 levels in HEK293 cells.
(**A**) Schematic diagrams of human KDM6B and C-terminal KDM6B proteins. Numbers in the diagrams correspond to the position of amino acid (AA) residues. JmjC, jumonji C domain. Red plus indicates the mutation of histidine at 1390 position into alanine. (**B**) Immunostaining analysis of Flag-KDM6B, Flag-KDM6B-C, and H3K27me3 in transfected HEK293 cells. Scale bar, 50 μm.

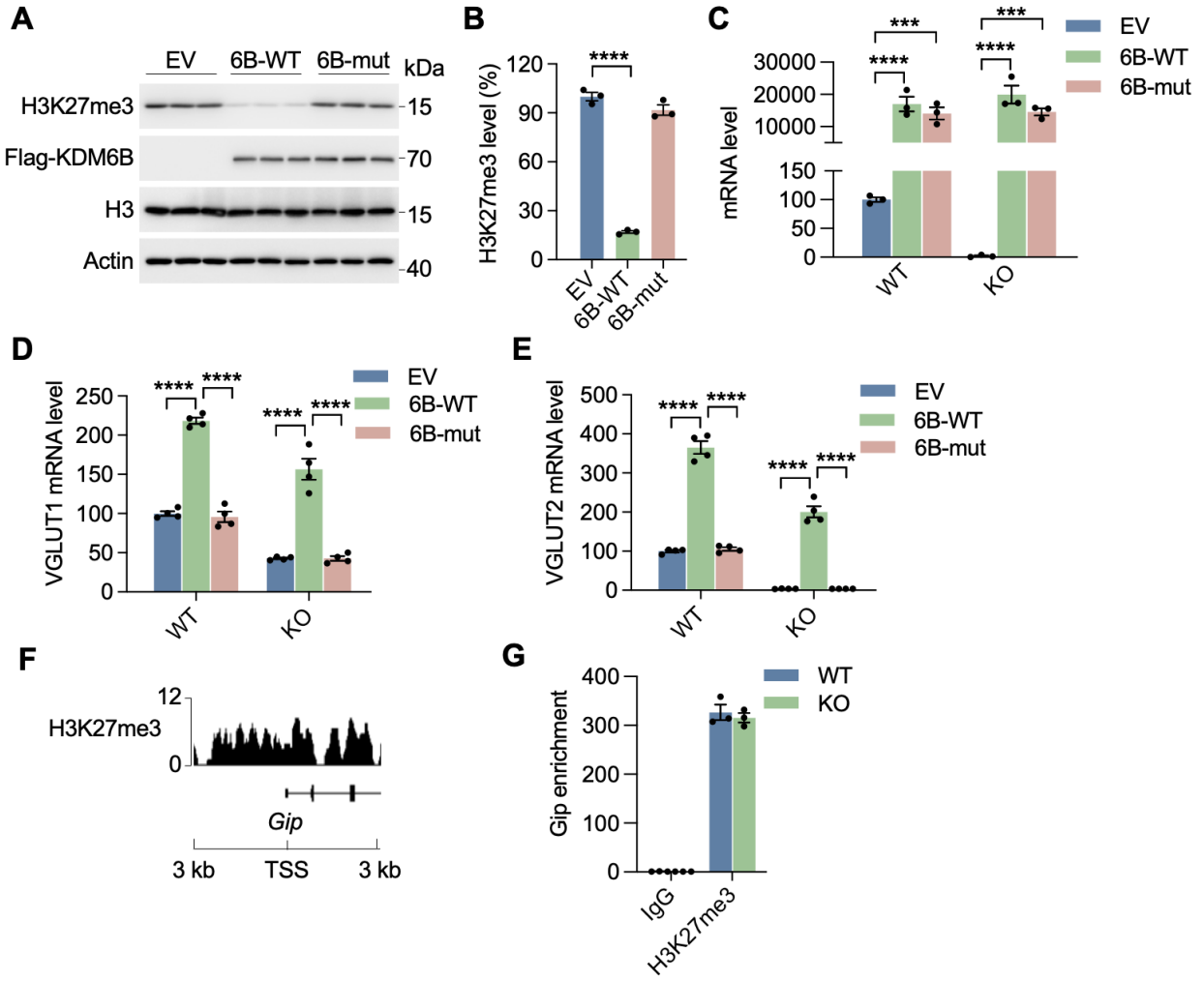

Fig. S7. KDM6B upregulates the expression of VGLUT1 and VGLUT2 through its demethylase activity.

(**A**, **B**) Immunoblot analysis (**A**) of H3K27me3 levels in neurons overexpressing of wild-type KDM6B (6B-WT) or catalytically inactive KDM6B mutant (6B-mut). The intensity of H3K27me3 bands was quantified and normalized to β-actin (**B**). n = 3 biological replicates in each group. Values of empty vector (EV) group were taken as 100%. One-way ANOVA with Tukey's multiple comparisons test. (**C**-**E**) qRT-PCR analysis of KDM6B (**C**), VGLUT1 (**D**), and VGLUT2 (**E**) mRNAs in KDM6B KO and WT neurons overexpressing of 6B-WT or 6B-mut. Values of EV group were taken as 100%. n = 4 biological replicates in each group. Two-way ANOVA with Sidak's multiple comparisons test for c and Tukey's multiple comparisons test for D and E. (**F**) H3K27me3 ChIP-seq peaks at the transcriptional start site (TSS; ±3 kb) of *Gip* in neurons. Data were retrieved from GSM2800528. (**G**) ChIP-qPCR analysis of H3K27me3 at the promoters of *Gip* in WT and KDM6B KO neurons (DIV18). n = 3 biological replicates in each group. Data were presented as mean ± s.e.m. ***p < 0.001; ****p < 0.0001.

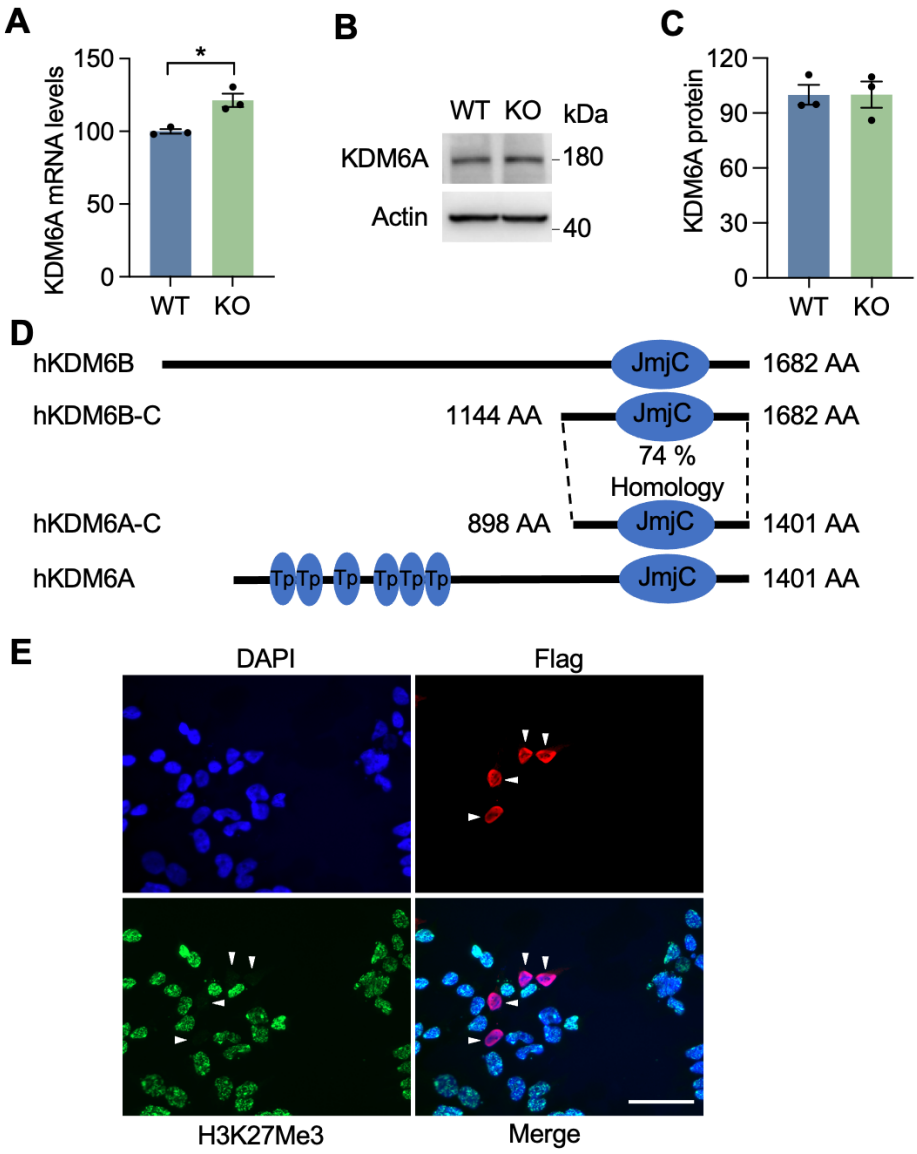

Fig. S8. C-terminal KDM6A is sufficient to reduce H3K27me3 levels in HEK293T cells. (**A**) qRT-PCR of KDM6A mRNA expression in KDM6B KO and WT neurons. Values of WT neurons were taken as 100%. $n = 3$ biological replicates in each group. Two-tailed Student's t test. (**B**, **C**) Immunoblot analysis of KDM6A in KDM6B KO and WT neurons. Representative images (**B**). The intensity of KDM6A bands was quantified and normalized to β-actin (**C**). $n = 3$ biological replicates in each group. Values of WT group were taken as 100%. (**D**) Schematic diagrams of human KDM6A, KDM6B, and C-terminal KDM6A and KDM6B proteins. Numbers in the diagrams correspond to the positions of amino acid (AA) residues. Tp, tetratricopeptide repeat; JmjC, jumonji C domain. (**E**) Immunostaining analysis of Flag-KDM6A-C and H3K27me3 in transfected HEK293T cells. Scale bar, 50 μm. Data were presented as mean ± s.e.m. *$p < 0.05$.

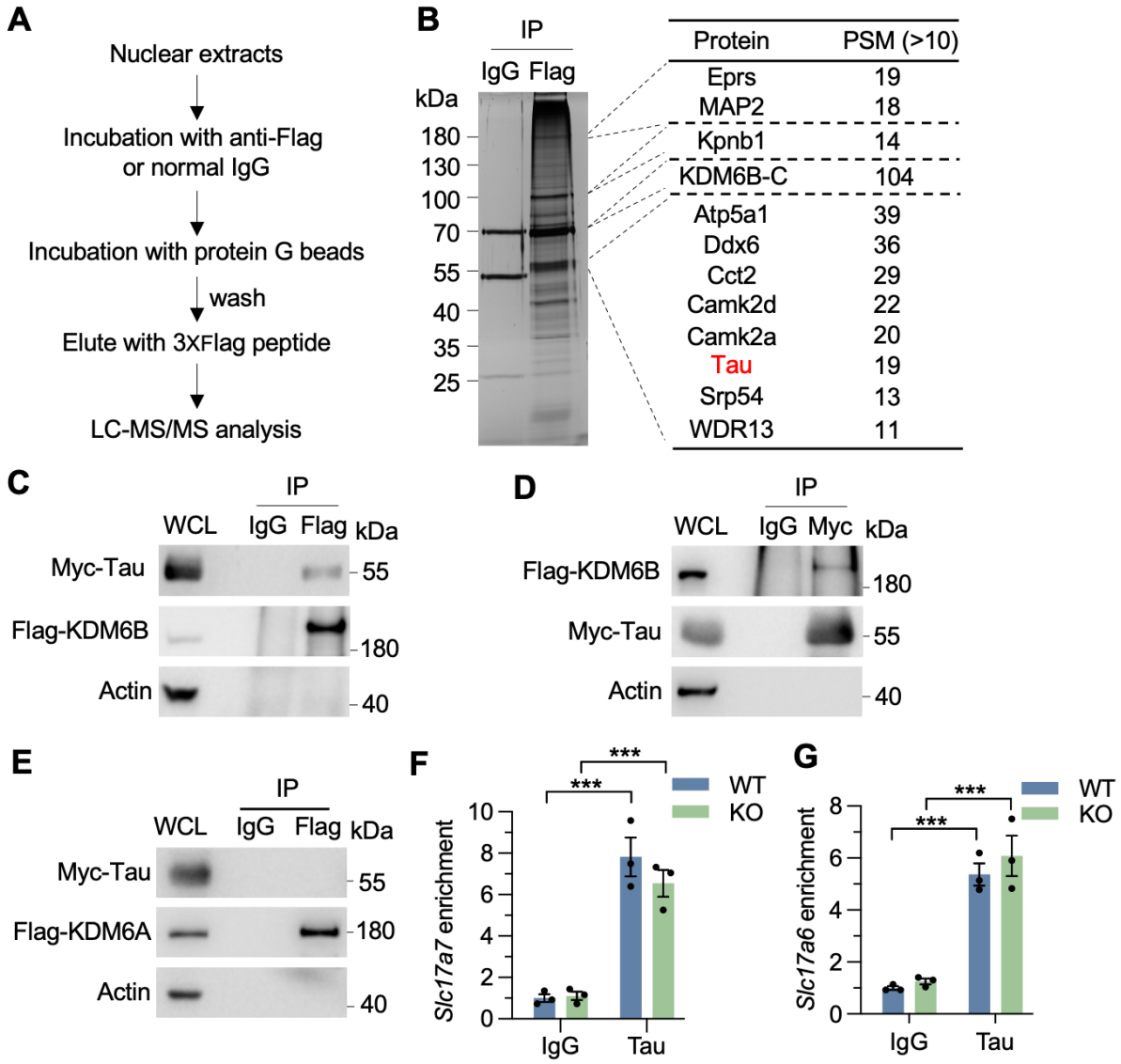

Fig. S9. Tau is a coregulator for KDM6B.

(**A**) Schematic diagram of mass spectrometry (MS) screening of KDM6B-interacting proteins. (**B**) Identification of KDM6B-interacting proteins in neurons. Sliver staining of KDM6B-interacting proteins (*left*). A list of top KDM6B-interacting proteins with peptide-spectrum match (PSM) score > 10 is shown (*right*). (**C**) Co-IP of Flag-KDM6B and Myc-Tau in transfected HEK293T cells with anti-Flag antibody. (**D**) Co-IP of Myc-Tau and Flag-KDM6B in transfected HEK293T cells with anti-Myc antibody. (**E**) Co-IP of Flag-KDM6A and Myc-Tau in transfected HEK293T cells with anti-Flag antibody. (**F**, **G**) ChIP-qPCR analysis of Tau at the promoters of *Slc17a7* (**F**) and *Slc17a6* (**G**) in WT and KDM6B KO neurons (DIV18). $n = 3$ biological replicates in each group. Two-way ANOVA with Tukey's multiple comparisons test. Data were presented as mean ± s.e.m. ***$p < 0.001$.

Supplementary Table 1. The list of antibodies used in this paper

Antibodies (dilutions)	Source	Catalog
anti-GluA1 (1: 1,000)	Millipore	MAB2263
anti-GluA2 (1: 1,000)	Millipore	MAB397
anti-GluN1 (1: 1,000)	Cell Signaling Technology	5704s
anti-GluN2A (1: 1,000)	Proteintech	19953-1-AP
anti-GluN2B (1: 1,000)	Cell Signaling Technology	14544s
anti-PSD95 (1: 1,000)	Millipore	MAB1598
anti-VGLUT1 (1: 10,000)	Synaptic Systems	135304
anti-VGLUT2 (1: 10,000)	Synaptic Systems	135404
anti-Synaptophysin (1: 1,000)	Cell Signaling Technology	36406s
anti-Brdu (1: 500)	Abcam	ab6326
Anti-Ki67 (1: 200)	ThermoFisher	MA5-14520
anti-Doublecortin (1: 500)	Santa Cruz Biotechnology	sc-8066
anti-Histone H3 (1: 5,000)	Cell Signaling Technology	4620s
anti-H3K27Me3 (1: 1,000)	Cell Signaling Technology	9733s
Anti-KDM6A (1: 1,000)	Cell Signaling Technology	33510s
anti-NeuN (1: 1,000)	Millipore	ABN90
anti-GFAP (1: 1,000)	DAKO	M0761
anti-Iba1 (1: 1,000)	Wako	019-19741
anti-MAP2 (1: 1,000)	Millipore	AB5622
anti-Tau (1: 1,00)	ThermoFisher	PA5-27287 (For ChIP)
anti-Tau (1: 1,000)	ThermoFisher	MA5-12808 (For IF)
anti-Flag (1: 10,000)	Sigma	F3165
anti-β-actin (1: 10,000)	Proteintech	66009-1-Ig
anti-Myc (1: 5,000)	Cell Signaling Technology	2278

Anti-Myc (1: 200)	Santa Cruz Biotechnology	SC-40 (For IP)
Anti-GFP (1: 1,000)	Aves Labs	GFP-1010

Supplementary Table 2. Oligonucleotide sequence used for qPCR primers

KDM6A	Forward: 5'- GGTCACTTCAACCTCTTATTGG -3'
	Reverse: 5'- CGACATAAAGCACCTCCTGA -3'
KDM6B	Forward: 5'- ATCCGAGGAACCAGACAGCACT -3'
	Reverse: 5'- GAGCATGTTGCCTGTGGATG -3'
VGLUT1	Forward: 5'- CCCTCGTCGCTACATCATCG -3'
	Reverse: 5'- GGGTTGTGCTGTTGTTGACC -3'
VGLUT2	Forward: 5'- GCCATCTCCTTCTTGGTGCT -3'
	Reverse: 5'- CTGCCATTCTTCACGGGACT -3'
SYP	Forward: 5'- CAGTTCCGGGTGGTCAAGG -3'
	Reverse: 5'- ACTCTCCGTCTTGTTGGCAC -3'
PSD95	Forward: 5'- GTGACAACCAAGAAATACCGCT -3'
	Reverse: 5'- TCACCTGCAACTCATATCCTGG -3'
Tau	Forward: 5'- CGTCCCTGGAGGAGGGAATA -3'
	Reverse: 5'- CTGAGGTGCCGTGGAGATG -3'
NeuN	Forward: 5'- ACGATCGTAGAGGGACGGAA -3'
	Reverse: 5'- CAGGGTTTAGCTTCCAGCCA -3'
Iba1	Forward: 5'- TCCGAGGAGACGTTCAGCTA -3'
	Reverse: 5'- GACCAGTTGGCCTCTTGTGT -3'
GFAP	Forward: 5'- CGGAGACGCATCACCTCTG -3'
	Reverse: 5'- AGGGAGTGGAGGAGTCATTCG -3'

Supplementary Table 3. Oligonucleotide sequence used for ChIP-qPCR

VGLUT1	Forward: 5'- AAGAGCTTGGAACGTGCAGA -3'
	Reverse: 5'- TCCTAGAGCCTCCACCTGTC -3'
VGLUT2	Forward: 5'- CGGGAGCGGTCAGGTTTTAT -3'
	Reverse: 5'- GCAGAGTGGCAGAGTGGAAT -3'
Gip	Forward: 5'- CTGTGCCCAGGAAAGAAGAG -3'
	Reverse: 5'- GGCTGTGCTAATGGGTGATT -3'

References

1. Casanova E, Fehsenfeld S, Mantamadiotis T, Lemberger T, Greiner E, Stewart AF *et al.* A CamKIIalpha iCre BAC allows brain-specific gene inactivation. *Genesis* 2001; **31**(1)**:** 37-42.

2. Dragatsis I, Zeitlin S. CaMKIIalpha-Cre transgene expression and recombination patterns in the mouse brain. *Genesis* 2000; **26**(2)**:** 133-135.

3. Wang Y, An R, Umanah GK, Park H, Nambiar K, Eacker SM *et al.* A nuclease that mediates cell death induced by DNA damage and poly(ADP-ribose) polymerase-1. *Science* 2016; **354**(6308).

4. Wang Y, Luo W, Reiser G. Activation of protease-activated receptors in astrocytes evokes a novel neuroprotective pathway through release of chemokines of the growth-regulated oncogene/cytokine-induced neutrophil chemoattractant family. *Eur J Neurosci* 2007; **26**(11)**:** 3159-3168.

5. Wang Y, Luo W, Stricker R, Reiser G. Protease-activated receptor-1 protects rat astrocytes from apoptotic cell death via JNK-mediated release of the chemokine GRO/CINC-1. *J Neurochem* 2006; **98**(4)**:** 1046-1060.

6. Lian H, Roy E, Zheng H. Protocol for Primary Microglial Culture Preparation. *Bio Protoc* 2016; **6**(21).

7. Liu S, Zhou M, Ruan Z, Wang Y, Chang C, Sasaki M *et al.* AIF3 splicing switch triggers neurodegeneration. *Mol Neurodegener* 2021; **16**(1)**:** 25.

8. Wang YN, Figueiredo D, Sun XD, Dong ZQ, Chen WB, Cui WP *et al.* Controlling of glutamate release by neuregulin3 via inhibiting the assembly of the SNARE complex. *Proc Natl Acad Sci U S A* 2018; **115**(10)**:** 2508-2513.

9. Chen Y, Zhang B, Bao L, Jin L, Yang M, Peng Y *et al.* ZMYND8 acetylation mediates HIF-dependent breast cancer progression and metastasis. *J Clin Invest* 2018; **128**(5)**:** 1937-1955.

10. Khandelwal N, Cavalier S, Rybalchenko V, Kulkarni A, Anderson AG, Konopka G *et al.* FOXP1 negatively regulates intrinsic excitability in D2 striatal projection neurons by promoting inwardly rectifying and leak potassium currents. *Mol Psychiatry* 2021; **26**(6)**:** 1761-1774.

11. Ruan Z, Lu Q, Wang JE, Zhou M, Liu S, Zhang H *et al.* MIF promotes neurodegeneration and cell death via its nuclease activity following traumatic brain injury. *Cell Mol Life Sci* 2021; **79**(1)**:** 39.

12. Can A, Dao DT, Terrillion CE, Piantadosi SC, Bhat S, Gould TD. The tail suspension test. *J Vis Exp* 2012; (59)**:** e3769.

13. Blazquez G, Castane A, Saavedra A, Masana M, Alberch J, Perez-Navarro E. Social Memory and Social Patterns Alterations in the Absence of STriatal-Enriched Protein Tyrosine Phosphatase. *Front Behav Neurosci* 2018; **12:** 317.

14. Leger M, Quiedeville A, Bouet V, Haelewyn B, Boulouard M, Schumann-Bard P *et al.* Object recognition test in mice. *Nat Protoc* 2013; **8**(12)**:** 2531-2537.